CHI3L1 Enhances Melanoma Lung Metastasis via Regulation of T cell Co-stimulators and CTLA-4/B7 Axis

Bing Ma[1,#], Suchitra Kamle[1,#], Bedia Akosman[1], Hina Khan[2], Chang Min Lee[1]
Chun Geun Lee[1], Jack A. Elias[1,3]

[1]Molecular Microbiology and Immunology
Brown University
185 Meeting St.
Providence, RI. 02912, USA

[2]Warren Alpert Medical School, Brown University and
Lifespan Cancer Institute, Providence, RI, 02912

[3]Department of Medicine
Brown University
Providence, RI 02912, USA

[#]Equal contribution

[5]**Corresponding author**: jack_elias@brown.edu

Running Title: CHI3L1 stimulates CTLA-4

Keywords: Chitinase 3-like-1, melanoma, metastasis, ICOS, ICOSL, CTLA-4, B7-1, B7-2, CD28, anti-CHI3L1, bispecific antibodies

Acknowledgements: This work was supported by National Institute of Health (NIH) grants PO1 HL114501(JAE), and R01 HL155558 (CGL) from NHLBI.

Competing Interests: JAE is a cofounder of Elkurt Therapeutics and is a stockholder of, and serves on the Scientific Advisory Board for Ocean Biopharma, Inc., which develops inhibitors of 18 glycosyl hydrolases as therapeutics. JAE, CGL and SK have composition of matter and use patents relating to antibodies against CHI3L1. The other authors have declared that no conflict of interest exists.

Author Contributions: Conception and design: BM, CGL, JAE, CGL; Generation of experimental resources and data collection: BM, SK, BA, HK, CML; Analysis and interpretation: BM, SK, CGL, JAE; Drafting the manuscript for important intellectual content: BM, CGL, JAE

Total Word Count: 27,360

ABSTRACT

ICOS and ICOSL and CD28 and B7 moieties are T cell co-stimulators and CTLA-4 is an immune checkpoint inhibitor. Chitinase 3-like-1 (CHI3L1) is induced in cancers where it portends a poor prognosis and contributes to metastasis. Here we demonstrate that, in pulmonary metastasis, CHI3L1 inhibits ICOS, ICOSL and CD28 while stimulating CTLA-4 and B7s. We also demonstrate that RIG-like helicase immune activation augments T cell co-stimulation while inhibiting CTLA-4 and pulmonary metastasis. At least additive antitumor responses were seen in metastasis models treated with individual antibodies against CTLA-4 and CHI3L1. Synergistic cytotoxic T cell-induced tumor cell death and the induction of the tumor suppressor PTEN were seen in co-cultures of T and tumor cells treated with bispecific antibodies that simultaneously target CHI3L1 and CTLA-4. Thus, CHI3L1 contributes to pulmonary metastasis by inhibiting T cell co-stimulation and stimulating CTLA-4. The simultaneous targeting of CHI3L1 and CTLA-4 with individual and, more powerfully with bispecific antibodies, represent promising therapeutic strategies for pulmonary metastasis.

.

Introduction

Neoantigens are generated during the development and progression of many cancers (Schumacher and Schreiber, 2015). In the majority of circumstances, the new antigens are recognized as “non-self” allowing the host to mount T cell-mediated “non self” immune responses that can control and or kill tumor cells (Schumacher and Schreiber, 2015). The T cell activation that occurs during these responses requires 2 signals. The first (signal 1), is provided by the interaction of the antigen/peptide with the T cell receptor (TCR) and major histocompatibility complex II (MHC II) on the surface of the antigen presenting cell (APC). The second is an antigen-independent co-stimulation which is mediated by moieties such as ICOS and ICOS ligand (ICOSL) and CD28 and its ligands B7-1 and B7-2 (also called CD80 and CD86). T cell activation is also highly regulated by immune checkpoints (ICP) that are regulated by inhibitory receptors and their ligands such as programed death (PD)-1 and its ligands PD-L1 and PD-L2; cytotoxic T lymphocyte antigen 4 (CTLA-4) and its ligands B7-1 and B7-2; and lymphocyte activation gene 3 protein (LAG3) and its ligand HLA class II (Nguyen and Ohashi, 2015). These are important findings because it is now known that cancers activate ICP pathways to inhibit host anti-tumor responses (Marcucci et al., 2017; Xu et al., 2014). In addition, immune checkpoint molecule blocking antibodies against PD-1, PD-L1, and CTLA-4 have proven to be successful therapeutics for a number of malignancies (Nguyen and Ohashi, 2015; Topalian et al., 2015). However, the moieties that regulate the expression of co-stimulators and ICPI have not been adequately defined.

CTLA-4 is a homodimeric glycoprotein receptor that is related to CD28. It is expressed on T cells within 1 hour of antigen exposure (Zhao et al., 2018) and inhibits T cell signaling by out-competing CD28 for binding to B7-1 and B7-2. It is also constitutively expressed on the surface of regulatory T cells (T regs) where it is required for contact-mediated immunosuppression (Rudd, 2009). Antibodies against CTLA-4 diminish tumor growth in murine

neoplastic modeling systems (Qin et al., 2019) and are effective as mono therapies in advanced melanoma, colorectal and renal cell cancers (Zhao et al., 2018). However, the processes that regulate the production of CTLA-4 have not been adequately defined.

Chitinase 3-like-1 (CHI3L1; also called YKL-40), the prototypic chitinase-like protein (CLP) is expressed by a variety of cells including macrophages, neutrophils and epithelial cells and is stimulated by a variety of inducers of injury, remodeling or inflammation (Lee et al., 2011). Studies from our laboratory and others have also demonstrated that CHI3L1 is a multifaceted moiety that inhibits cell death (apoptosis and pyroptosis), stimulates Th2 inflammation and M2 macrophage differentiation, inhibits oxidant injury, controls inflammasome and caspase activation, regulates TGF-β1 elaboration, contributes to antibacterial responses and activates MAP Kinase (MAPK), Akt/Protein Kinase B and Wnt/β-catenin signaling (Dela Cruz et al., 2012; He et al., 2013; Kanneganti et al., 2011; Lee et al., 2009; Sohn et al., 2010). Elevated levels of CHI3L1 have been noted in a wide variety of diseases characterized by inflammation, fibrosis and tissue remodeling (Lee et al., 2011; Libreros and Iragavarapu-Charyulu, 2015; Matsuura et al., 2011; Ober et al., 2008; Zhou et al., 2015). The levels of circulating CHI3L1 are also increased in cancers of the prostate, colon, lung, rectum, ovary, kidney, breast, glioblastomas and malignant melanoma where they frequently correlate directly with disease progression and inversely with disease-free interval and survival (Chen et al., 2011; Choi et al., 2010; Iwamoto et al., 2011; Johansen et al., 2009; Junker et al., 2005; Peng et al., 2010; Schmidt et al., 2006; Shao et al., 2011; Thom et al., 2010). CHI3L1 may also play a particularly important role in pulmonary metastasis where studies from our laboratory and others have demonstrated that CHI3L1 induction is required for the generation of a metastasis permissive pulmonary microenvironment (Ma et al., 2015) and metastatic spread can be inhibited via RIG-like helicase (RLH) innate immune inhibition of CHI3L1 elaboration (Ma et al., 2016). Our studies also demonstrated that CHI3L1 is a potent stimulator of the PD-1-PD-L1/2 immune checkpoint inhibitor pathway (Ma et al., 2021). However, the mechanism(s) by which

CHI3L1 contributes to tumor initiation and spread have not been fully defined and the degree to which CHI3L1 mediates its tumorigenic effects via activating T cell co-stimulators and or the CTLA-4-B7 axis have not been addressed. In addition, although recent studies reported that RLH activation is critical for responsiveness to immune checkpoint blockade (Ma et al., 2021), the possibility that this responsiveness is mediated by RLH immune inhibition of CHI3L1 has not been addressed.

We hypothesized that CHI3L1 contributes to pulmonary metastasis via the regulation of T cell co-stimulation and inhibitory ICP. To address this hypothesis, studies were undertaken to determine if CHI3L1 regulates co-stimulatory and or ICP pathways. These studies demonstrate that CHI3L1 inhibits ICOS, ICOS ligand (ICOSL) and CD28 while stimulating B7-1, B7-2 and CTLA-4. They also demonstrate that RLH innate immune activation augments co-stimulation, inhibits CTLA-4 and suppresses pulmonary metastasis. At least additive antitumor effects were seen in murine metastasis models treated simultaneously with individual antibodies against CTLA-4 and CHI3L1. Synergistic cytotoxic T cell (CTL)-induced tumor cell death and the induction of the tumor suppressor PTEN were seen in T cell-tumor co-cultures treated with bispecific antibodies that simultaneously target CHI3L1 and CTLA-4. These studies demonstrate that CHI3L1 contributes to the development and or progression of metastatic tumors in the lung via the regulation of co-stimulation and CTLA-4-mediated immunosuppression. They also strongly support the concept that the simultaneous inhibition of CHI3L1 and CTLA-4 with monospecific antibodies and, even more powerfully with bispecific antibodies, represent novel and attractive therapeutic strategies for lung metastasis.

Results

Pulmonary melanoma metastasis inhibits the Costimulators ICOS, ICOSL and CD28.

Studies were undertaken to determine if the expression of T cell costimulators such as ICOS and ICOSL was altered by the metastatic spread of melanoma to the lung. In these experiments, 8

weeks old C57BL/6 mice were challenged with freshly prepared B16-F10 (B16) melanoma cells or vehicle control and the pulmonary expression of ICOS, ICOSL and CD28 were evaluated 2 weeks later. These studies demonstrated that melanoma metastasis was associated with significant inhibition of the expression of ICOS and ICOSL (Fig. 1, A and B). This induction was not specific for the ICOS moieties because the levels of mRNA encoding CD28 were also reduced (Fig. 1 C). In all cases, these changes in mRNA were associated with comparable alterations in the levels of costimulatory proteins (Fig. 1 D). They were prominent in CD11b+ and SPC+ cells (Fig. 1, E and F; Fig. S1, A and B). When viewed in combination, these studies demonstrate that pulmonary melanoma metastasis is associated with significantly suppressed expression of T cell co-stimulators including ICOS, ICOSL and CD28.

Pulmonary melanoma metastasis stimulates CTLA-4 and its ligands.

Studies were next undertaken to determine if the expression of ICPI, such as CTLA-4, were altered by the metastatic spread of melanoma to the lung. In these experiments, 8 weeks old C57BL/6 mice were challenged with freshly prepared B16-F10 (B16) melanoma cells or vehicle control and the pulmonary expression of CTLA-4 was evaluated 2 weeks later. These studies demonstrated that melanoma metastasis was associated with significant stimulation of CTLA-4 and its ligands B7-1 and B7-2 (Fig. 2, A-C). These alterations in gene expression were associated with comparable alterations in the levels of CTLA-4 and its B7 ligands (Fig. 2D) that could be readily appreciated in CD11b+ and CD3+ cells and, to a lesser extent, SPC+ and CC10 + cells (Fig. 2, E and F; Fig. S1, C and D and Fig. S2 A). This induction was not specific for the CTLA-4 because PD-1 and PD-L1 were similarly induced as described by our laboratory (Ma et al., 2021). It was also not specific for ligands of B7-1 and or B7-2 because CD28, which also binds these moieties, was inhibited in this setting as noted above. These studies demonstrate that pulmonary melanoma metastasis is associated with significantly enhanced expression of CTLA-4 and B7-1 and B7-1.

CHI3L1 plays an important role in in melanoma metastasis inhibition of co-stimulation and the induction of CTLA-4 and its ligands.

To begin to define the role(s) of CHI3L1 in the inhibition of co-stimulation and induction of CTLA-4 and its ligands, we compared the levels of ICOS, ICOSL, CD28, CTLA-4, B7-1 and B7-2 in wild type (WT) and CHI3L1 (*Chil1*) null mutant (*Chil1*$^{-/-}$) mice that were randomized to receive B16 cells or vehicle control. As can be seen in Fig. 3 in panels A and B, the inhibition of ICOS, ICOSL and CD28 and the stimulation of CTLA-4 and its ligands were abrogated in mice with null mutations of CHI3L1 (*Chil1*$^{-/-}$). In accord with these findings, B16 cell inhibition of ICOS, ICOSL and CD28 and stimulation of CTLA-4, B7-1 and B7-2 were also significantly diminished in lungs from mice treated with monoclonal anti-CHI3L1 antibody (called FRG antibody) (Fig. 3, C and D). In addition, the ability of B16-F10 cells to stimulate CTLA-4, B7-1 and B7-2 were further exaggerated in transgenic mice in which CHI3L1 was targeted to the lung (Fig. 3 E). When viewed in combination, these studies demonstrated that CHI3L1 plays an essential role in melanoma inhibition of T cell co-stimulation and the induction of CTLA-4 and its ligands.

Transgenic CHI3L1 inhibits co-stimulation and stimulates CTLA-4 and its ligands in the normal lung

The studies noted above demonstrate that pulmonary melanoma metastasis inhibit T cell co-stimulation and stimulate ICPI such as CTLA-4 and its ligands and that CHI3L1 plays a critical role in these inductive events. However, because null mutations of CHI3L1 and treatment with α-CHI3L1 neutralizing antibody decrease metastatic spread (Ma et al., 2015; Ma et al., 2016), the studies do not determine if the inhibition of ICOS and ICOSL and or the induction of CTLA-4 that are seen in CHI3L1 null mutant mice or mice treated with anti-CHI3L1 are due to the direct effects of CHI3L1 or the importance of CHI3L1 in melanoma metastatic spread. To address this issue, studies were undertaken to determine if CHI3L1 inhibits co-stimulation and stimulates the CTLA-

4 axis in the absence of B16 cell administration. In these experiments, we compared the expression and accumulation of ICOS, ICOSL CD28, CTLA-4, B7-1 and B7-2 in lungs from WT mice and transgenic mice (Tg) in which CHI3L1 was overexpressed in a lung-specific manner. These experiments demonstrated that CHI3L1 is a potent inhibitor of ICOS, ICOSL and CD28 and a stimulator of CTLA-4 and B7-1 and B7-2 mRNA and protein in lungs from Tg mice when compared to WT controls (Fig. 4, A-D). FACS evaluations and IHC demonstrated that transgenic CHI3L1 specifically stimulated CTLA-4 and B7-1 and B7-2 in a variety of cells including CD3+ T cells, macrophages, and epithelial cells (Fig. 4, D and E; Fig. S2 B). These studies demonstrate that the inhibition of ICOS, ICOSL and CD28 and stimulation of CTLA-4 and its ligands in pulmonary melanoma metastasis is mediated, at least in part, by a tumor-independent effect of CHI3L1.

Rig-like helicase (RLH) activation augments costimulation and inhibits CTLA-4, B7-1 and B7-2

We previously demonstrated that Poly(I:C), a strong activator of retinoic acid inducible gene I (RIG-I) and the RIG-like helicase (RLH) innate immune response, prominently inhibits CHI3L1 expression and melanoma lung metastasis (Ma et al., 2016). Recent studies also demonstrated that RIG-I activation and mitochondrial antiviral signaling molecule (MAVS) are essential for many immune checkpoint inhibitor blockade-induced anti-tumor responses (Heidegger et al., 2019). Thus, studies were undertaken to determine if RLH activation with Poly(I:C) altered the ability of CHI3L1 to inhibit ICOS, ICOSL and CD28 and stimulate CTLA-4 and its ligands. Poly(I:C) ameliorated melanoma- inhibition of ICOS, ICOSL and CD28 while abrogating the ability of B16 cells to stimulate CTLA-4 (Fig. 5, A and B). FACS analysis also demonstrated that T cell expression of CTLA-4 was prominently reduced while macrophage expression of CD28 was augmented by poly(I:C) treatment (Fig. 5, C and D). The stimulation of ICOS, ICOSL, and CD28 and inhibition of CTLA-4 and B7-1 and B7-2 by Poly(I:C) were at least partially dependent on

CHI3L1 because the transgenic overexpression of CHI3L1 using a promoter that is not regulated by the RLH pathway ameliorated Poly(I:C)-induced inhibition of the co-stimulators and ICPI stimulation (Fig. 6, A and B). These studies highlight the ability of RLH activation to inhibit CHI3L1 and, in turn, eliminate its ability to inhibit co-stimulation and augment the expression and accumulation of ICPI.

Anti-CHI3L1 and anti-CTLA-4 interact to augment antitumor responses in melanoma lung metastasis

Since CHI3L1 regulates co-stimulation and stimulates multiple ICPIs including CTLA-4, studies were undertaken to determine if anti-CHI3L1 and anti-CTLA-4 interact in inducing antitumor responses. In these experiments, mice were treated with the antibodies against CHI3L1 and CTLA-4, individually and in combination. As can be seen in Fig. 7, FRG and anti-CTLA-4 individually inhibited melanoma metastasis when compared to isotype controls (Fig. 7, A and B). Importantly, when mice were treated with 50 μg doses of the two antibodies in combination, the antitumor responses induced by the antibodies in combination exceeded the effects that were seen when the antibodies were used individually (Fig. 7, A and B). These effects appeared to be at least additive in nature. These studies demonstrate that anti-CHI3L1 and anti-CTLA-4 interact to augment antitumor responses in lung melanoma metastasis.

Bispecific antibodies that simultaneously target CHI3L1 and CTLA-4 synergistically induce CTL cell differentiation, PTEN expression and tumor cell death

In recent years it has become clear that combination therapy with ICP blockers can induce particularly potent responses in a variety of tumors including lung cancers (Hellmann et al., 2018; Motzer et al., 2018; Wolchok et al., 2017). Recent studies have also demonstrated that bispecific antibodies can have powerful and or unique biologic effects compared to their individual component antibodies, alone and in combination (Dahlen et al., 2018). The studies noted above

suggest that antibodies against CHI3L1 and CTLA-4 interact to enhance antitumor responses in melanoma metastasis. Thus, studies were undertaken to determine if bispecific antibodies that simultaneously target CHI3L1 and CTLA-4 (FRGxCTLA-4) elicit even more impressive antitumor responses. To address this question, we made bispecific antibodies in which anti-CTLA-4 was linked to FRG via its light chain (Fig. S3). This antibody, termed FRGxCTLA-4, manifest high affinities to both CHI3L1 and CTLA-4 (Kd=1.1×10^{-9}) that were comparable to the affinities of the individual antibody moieties (Fig. S3). We then compared the effects of FRGxCTLA-4 to FRG and anti-CTLA-4 alone and in combination, in vivo and in a coculture system containing activated T cells and A357 human melanoma cells. In the in vivo experiments the bispecific antibodies were impressively powerful inhibitors of melanoma metastasis (Fig. 7, A and B). These effects were synergistic in nature when compared to antibodies against CHI3L1 or CTLA-4 individually and more powerful than the antitumor effects that were seen when the individual antibodies were administered simultaneously (Fig. 7, A and B). In the co-culture experiments, FRG and anti-CTLA-4 individually caused a significant increase in tumor cell apoptosis (Fig. 8 A). When FRG and anti-CTLA-4 were administered simultaneously an additional increase in tumor cell death was seen. This effect appeared to be at least additive in nature (Fig. 8 A). Importantly the highest levels of tumor cell apoptosis were seen when the bispecific antibody FRGxCTLA-4 was employed (Fig. 8 A). This effect appeared to be synergistic in nature because the levels of tumor cell death that were seen greatly exceeded the effects of FRG and anti-CTLA-4 when administered individually or in combination. In all cases, the tumor cell death that was seen appeared to be mediated by CD8+ cytotoxic T cells because FRG and anti-CTLA-4, alone and in combination, heightened T cell expression of CD8, perforin and granzyme and these effects were synergistically enhanced in co-cultures treated with FRGxCTLA-4 (Fig. 8, B-D). Surprisingly, FRG and anti-CTLA-4, alone and in combination, also heightened the expression of the tumor suppressor PTEN and these effects were synergistically enhanced in co-cultures treated with FRGxCTLA-4 (Fig. 8 E). In quantitative evaluation, the anti-tumor effects of mono and bispecific

antibodies of FRG and CTLA-4 were all significant (Fig. 8 F). When viewed in combination, these studies demonstrate that bispecific antibodies that simultaneously target CHI3L1 and CTLA-4 have impressive, synergistic anti-tumor effects in vitro that are mediated by its ability to induce CD8+ cytotoxic T cells and enhance tumor cell expression of PTEN.

Discussion

The immune surveillance hypothesis proposed in the 1950's that the immune system could recognize and reject cancer cells as foreign (Topalian, 2017). It is now known that CD8+ cytotoxic T cells are the main players driving adaptive immune responses to cancer (Huff et al., 2019) and that tumors get shielded from immune elimination by decreasing T cell co-stimulation and or expressing ligands that normally interact with inhibitory immune receptors that protect "self" (Topalian, 2017). To further understand the mechanisms that mediate these immunosuppressive responses, we tested the hypothesis that CHI3L1 plays a critical role in these tumor inhibitory events. These studies highlighted the ability of pulmonary metastasis to inhibit T cell co-stimulation and induce CTLA-4 and its ligands. Interestingly, transgenic CHI3L1, in the absence of tumor, reproduced these events, demonstrating that the effects of CHI3L1 are, at least partially, tumor independent. These findings provide a potential mechanism(s) for the immunosuppressive effects of CHI3L1 that have been described in the context of breast cancer (Cohen et al., 2017). They also describe a potentially important mechanism by which type I immune responses can be coopted to shut down antitumor immune responses (Herbst et al., 2014; Nguyen and Ohashi, 2015). These studies also have important therapeutic implications because they demonstrate that the simultaneous administration of anti-CHI3L1 and anti-CTLA-4 antibodies generate, at least additive, antitumor responses *in vivo* and that bispecific antibodies that simultaneously target CHI3L1 and CTLA-4 synergistically induce CD8+ cytotoxic T lymphocyte differentiation and tumor cell death.

The CD28 costimulatory receptor is a 44kDa membrane glycoprotein that is expressed on nearly all human T cells at birth (Esensten et al., 2016). Binding of the CD28 receptor provides an essential second signal alongside TCR ligation which induces T cell activation (Huff et al., 2019). CD28 is the prototype of a family of co-stimulators that includes ICOS and others (Huff et al., 2019; Mahmoud et al., 2011). CD28 and CTLA-4 compete for the same ligands (B7-1 and B7-2). They regulate immune responses by providing opposite effects with CD28 stimulating and CTLA-4 inhibiting T cell function (Huff et al., 2019). In keeping with these findings, CD28 agonists have been developed that awaken T cells from a tolerant state and activate the immune system in the treatment of cancer and infection (Attanasio and Wherry, 2016; Callahan et al., 2016). Our studies add to our understanding of CD28 and related moieties by demonstrating, for the first time, that CHI3L11 plays a critical role in their regulation. Specifically, they demonstrate that CHI3L1 inhibits ICOS, ICOSL and CD28 co-stimulation while augmenting the expression of the immune inhibitor CTLA-4. This supports the concept that combining checkpoint inhibitors and agonists of co-stimulation represents an exciting therapeutic approach for cancer therapy (Emerson and Redmond, 2018). It also demonstrates how anti-CHI3L1-based interventions can have these desired multifaceted effects.

Programed cell death (PD)-1 and CTLA-4 are co-inhibitory receptors that inhibit T cell activity and, as such, are referred to as immune checkpoints (Zhao et al., 2019). Antibodies that block these receptors or their ligands have impressive clinical activity against an array of human cancers (Rotte, 2019; Seidel et al., 2018; Zhao et al., 2019). In addition, the combination of anti-CTLA-4 and an anti-PD-1 or anti-CTLA-4 and an anti-PD-L1 are far more effective than either agent alone in clinical trials (Callahan et al., 2016; Larkin et al., 2015) or pre-clinical models (Duraiswamy et al., 2014). In keeping with the importance of these interactions the mechanisms that underlie the interactions of CTLA-4 and the PD-1/PD-L1 axis have been studied. These recent investigations demonstrated that PD-L1 and CD80 (B7-1) bind to each other exclusively in *cis* and that this interaction blocks the immunosuppression induced by both the PD-1/PD-L1 axis

and the CTLA-4/B-7 axis while leaving CD28/B-7 T cell co- stimulation unaltered (Zhao et al., 2018). Our studies add to this mechanistic understanding by demonstrating that CHI3L1 stimulates both CTLA-4 and components of the PD-1/PD-L1 axis while simultaneously inhibiting ICOS and CD28 co-stimulation (Zhao et al., 2018). When viewed in combination one can appreciate the multifaceted manner via which ICP moieties interact to suppress antitumor immune responses.

Activation of the RIG-I/RLH signaling pathway in tumors and the host microenvironment has recently been demonstrated to be a critical component of immune checkpoint blockade (ICB) induced by antibodies against CTLA-4, alone and in combination with antibodies against PD-1 (Ma et al., 2021). Appropriately induced ICB triggers tumor cell death, presentation of tumor associated antigens by CD103+ dendritic cells and the accumulation of antigen specific CD8+ infiltrating T cells (Ma et al., 2021). It was speculated that nucleic acids leaking from disintegrating tumor cells are engulfed by host myeloid cells to induce RLH activation (Ma et al., 2021). We previously demonstrated that RLH activation powerfully inhibits CHI3L1 production (Ma et al., 2016). The present studies demonstrate that RLH inhibition of CHI3L1, in turn, augments T cell co-stimulation and inhibits the expression of CTLA-4. They also demonstrate that, at least additive, antitumor effects are seen when mice with melanoma metastasis are treated simultaneously with anti-CHI3L1 and anti-CTLA-4 individually and that synergistic tumor cell death responses are seen in tumor-T cell co-cultures treated with the bispecific antibody FRGxCTLA-4. These studies provide an additional mechanism that can explain how RIG-I/RLH activation fosters ICB antitumor responses. Specifically, they suggest that the antitumor effects of RIG-I/RLH activation are due to its ability to inhibit CHI3L1 and that CHI3L1 is a critical regulator of ICB. This raises the exciting possibility that interventions that inhibit or block CHI3L1 can be used to maximize the therapeutic efficacy of ICB.

Lung cancer is the leading cause of cancer-related mortality worldwide (Siegel et al., 2017). In keeping with its importance, scientists have focused on our knowledge of tumor

immunology and developed new therapeutics for patients with primary and metastatic lung malignancies (Topalian, 2017). In many cases these therapies are now first or second line lung cancer therapeutics (Santini and Hellmann, 2018). However, only a minority of patients responded to these therapies and the responses that have been seen were often not durable (Yang, 2015). To address these issues combination immunotherapy has been attempted. The simultaneous treatment with anti-PD-1 and anti-CTLA-4 has been most commonly employed (Rotte, 2019). This combination has engendered powerful effects in some malignancies. However, it has not proven successful in lung cancers. In addition, its use is limited by toxicities such as the pneumonitis that is caused by the exaggerated anti-self-immune responses that the antibody combination induces (Rotte, 2019). In keeping with the concept that combination immunotherapy may be therapeutically useful, we evaluated the effects of anti-CHI3L1 (FRG) and anti-CTLA-4, alone and in combination. These studies demonstrate that the simultaneous treatment with antibodies that target CHI3L1, and CTLA-4 individually results in at least additive antitumor responses. Based on our finding that RLH activation inhibits CHI3L1 we can also envision similarly augmented anticancer response if RLH activators and anti-CTLA-4 are co-administered. Whether the safety profile of these immunotherapeutic combinations is better or worse than anti-PD-1 plus anti-CTLA-4 will need to be determined.

Although antibody-based blockade of individual checkpoints has proven therapeutically useful in a variety of human cancers, the responses that are elicited are often not durable (Cohen and Flaherty, 2019). This is in keeping with recent observations that demonstrate that the blockade of a single checkpoint target can lead to the compensatory upregulation of other checkpoint receptors (Koyama et al., 2016; Qin et al., 2019). As a result, many have turned to combinations of therapeutics that target non-redundant immune pathways to achieve enhanced antitumor responses (Qin et al., 2019). Our studies support this concept by demonstrating that the combined use of antibodies that target CHI3L1 (a multifaceted stimulator of ICP) and CTLA-

4 results in enhanced antitumor responses. Additional investigation will be required to define the optimal combination of immune blockade antagonists for primary and metastatic lung cancer.

Bispecific antibodies are a growing class of immunotherapies with the potential to further improve clinical efficacy and safety (Dahlen et al., 2018). To address the possibility that bispecific antibodies that simultaneously target CHI3L1 and CTLA-4 might be particularly effective, bispecific antibodies were generated and their effects in a T cell-melanoma cell coculture system were evaluated and compared to individual antibodies, alone and in combination. These studies demonstrate that FRGxCTLA-4 was a remarkably effective inducer of tumor cell death. They also demonstrated that these antitumor responses were synergistic when compared to the effects of the individual antibodies. Lastly, they demonstrated that the tumor cell death responses were due to the ability of FRGxCTLA-4 to induce CD8+, perforin +, and granzyme+ cytotoxic T cells. These findings agree with a fundamental principle of tumor immunology, that cancer cells can be eliminated by host cytotoxic T cells (Pfirschke et al., 2016). The synergistic nature of the responses induced by FRGxCTLA-4 further support our contention that multiple different immunoregulatory pathways are involved in this response. Specifically, they demonstrate that interventions that diminish the production and or effector functions of CHI3L1 inhibit the ability of CHI3L1 to block cell death (apoptosis and pyroptosis) and augment the accumulation of IFNα/β, chemerin and its receptor ChemR23, phosphorylated cofilin and LimK2 (Ma et al., 2016). CHI3L1-based interventions also augment the expression of the tumor suppressor PTEN, and decrease M2 macrophage differentiation and augment type I immune responses (Ma et al., 2016). When viewed in combination, these studies demonstrate that bispecific antibodies that simultaneously target CHI3L1 and CTLA-4 have impressive synergistic antitumor effects while simultaneously inducing CD8+ CTL differentiation and tumor cytotoxicity.

In conclusion, these studies demonstrate that CHI3L1 inhibits the T cell co-stimulation induced by ICOS and CD28 and their ligands while stimulating the checkpoint inhibitor CTLA-4. They also demonstrate that the simultaneous treatment of pulmonary metastatic melanoma with

individual antibodies against CHI3L1 or CTLA-4 generates an additive antitumor response and that bispecific antibodies that simultaneously target CHI3L1 and CTLA-4 synergistically induce CD8+CTL-induced tumor cell death. These findings predict that interventions that simultaneously target CHI3L1 can augment the efficacy of immune checkpoint blockade in response to anti-CTLA-4 in lung cancer and potentially other malignancies. Additional investigations of the biology and therapeutic consequences of interactions between CHI3L1 and immune checkpoint inhibitors are warranted.

Materials and methods

Genetically modified mice

Mice with null mutations of CHI3L1 *(Chil1$^{-/-}$)* and transgenic mice in which human CHI3L1 was targeted to the lung with the CC10 promoter (*Chi3l1 Tg*) have been generated and characterized by our laboratory as previously described (Lee et al., 2009; Lee et al., 2016). All animals were humanely anesthetized with Ketamine/Xylazine (100mg/10mg/kg/mouse) before any intervention. The protocols that were used in these studies were evaluated and approved by the Institutional Animal Care and Use Committee (IACUC) at Brown University.

Western blot analysis

20 to 40 µg of total lung lysates were prepared with RIPA lysis buffer (ThermoFisher Scientific, Waltham, MA, USA) and subjected to the evaluations according to the procedures that we recently reported (Ma et al., 2021). Anti-mouse ICOS (7E.17G9, Bio X Cell) and anti-mouse ICOSL (HK5.3, Bio X Cell), anti-mouse CD28 (37.51, Bio X Cell), anti-human-CTLA-4 (922101, R&D), anti-mouse-CTLA-4 (a generous gift from Prof. Lieping Chen, Medical Oncology, Yale School of Medicine), anti-mouse B7-1 (F-7, Santa Cruz Biotechnology) and anti-mouse B7-2 (BU63, Santa Cruz Biotechnology) and β-actin (C4, Santa Cruz Biotechnology) were used as

primary antibodies and immunoreactive bands were detected by using a ChemiDoc (Bio-Rad) imaging system.

RNA extraction and Real-time qPCR

Total lung mRNA was isolated using TRIzol reagent (ThermoFisher Scientific) followed by RNA extraction using RNeasy Mini Kit (Qiagen, Germantown, MD) according to the manufacturer's instructions. mRNA was measured and used for real time (RT)-PCR as described previously (Lee et al., 2009; Sohn et al., 2010). The primer sequences used in these studies are summarized in Table S1. Ct values of the test genes were normalized to the internal housekeeping gene β-actin.

Generation of α-CHI3L1 and humanized bispecific antibodies against CHI3L1 and CTLA-4

The murine monoclonal anti-CHI3L1 antibody (FRG) was generated as described previously (Ma et al., 2021). CHI3L1 (FRG) x CTLA-4 bispecific antibodies were generated with Fc portion of FRG antibody (IgG1 isotype) in which anti-CTLA-4 was linked to FRG via its light chain (Fig. S3). HEK-293T cells were transfected with the bivalent FRGxCTLA-4 construct using Lipofectamine™ 3000 (Invitrogen # L3000015, CA, USA). Supernatant was collected for 7 days, and the antibody was purified using a protein A column (Thermo scientific # 89960; IL, USA). Ligand binding affinity and sensitivity were assessed using ELISA techniques. The original murine anti-CTLA-4 monoclonal antibody (Dong et al., 2002) was a generous gift from Prof. Lieping Chen (Medical Oncology, Yale School of Medicine). At the end of the preparation of the bispecific antibody endotoxin levels were below the limits of detection of the Limulus Amebocyte Assay (Pierce, Rockford IL).

Melanoma lung metastasis and antibody treatment

B16-F10, a mouse melanoma cell line, was purchased from ATCC (Cat#: CRL-6475, Manassas, VA) and maintained in Dulbecco's Modified Eagles Medium (DMEM) supplemented with 10% Fetal bovine Serum (FBS) and 1% penicillin & streptomycin as recommended. As previously described, intraperitoneal injection of the noted doses of anti-CHI3L1 (FRG) and anti-CTLA-4, alone and in combination and bispecific CTLA-4 antibody and isotype control IgG (IgG2b) were started on the day of the B16 tumor cell challenge and continued every other day for 2 weeks (Ma et al., 2015; Ma et al., 2016). Metastasis was assessed and quantified by counting the melanoma colonies (black dots) on the pleural surface as previously described (Ma et al., 2015; Ma et al., 2016).

Fluorescence-activated cell sorting (FACS) analysis

Single cell suspensions from whole mouse lungs were prepared using the lung dissociation kit (Miltenyi Biotec, Auburn, CA) as per the manufacturer's instructions. Cells were stained with fluorescently labeled antibodies directed against CD45 (30-F11, Fisher Scientific), CC10 (E-11, Santa Cruz Biotechnology), SPC (H-8, Santa Cruz Biotechnology), CD3-APC (145-2C1, Fisher Scientific), CD11b-FITC (M1/70, Fisher Scientific), MHC-II (M5/114.15.2, Fisher Scientific), ICOS-PE-cy7 (C398.4A, Biolegend), CD28-PE-cy7 (25-0289-42, ebioscience), and CTLA-4-PE-cy7 (25-1522-82, ebioscience). Flow cytometry data was collected using the BD FACSAria IIIu and analyzed with FlowJo V10 software.

Immunohistochemistry

Formalin-fixed paraffin embedded (FFPE) lung tissue blocks were serially sectioned at 5μm-thickness and were subjected to immunohistochemistry (IHC) evaluations according to the procedures that we recently reported (Ma et al., 2021). The primary antibodies used in this IHC evaluations are: α-CTLA-4 (a generous gift from Prof. Lieping Chen, Medical Oncology, Yale

School of Medicine), α-CC10 (E-11, Santa Cruz Biotechnology), α-SPC (M-20, Santa Cruz Biotechnology), and α-CD68 (#ab125212, abcam).

Melanoma cells and TALL-104 T cell co-cultures

TALL-104 T cells (CRL-11386) and human melanoma A375 cell line (CRL-1619) were purchased from ATCC and cultured according to the instructions provided by the vendor. The TALL-104 cells were activated by incubating them with anti-human CD3 antibody (5μg/ml) (Biolegend) and anti-human CD28 antibody (5μg/ml) (#MABF408, Millipore). After incubation, the cells were washed and B16 melanoma and activated TALL-104 cells were resuspended together at a 1: 6 ratio in complete RPMI media, dispensed into the multi-well slide chambers and incubated in 5% CO2 and air at 37˚C. One hour later, the co-cultured cells were treated with the isotype control antibody or test antibodies. The effects of the isotype control antibodies were compared to the effects of antibodies against CHI3L1 (FRG; 5μg), CTLA-4 (5μg), FRG+CTLA-4 administered simultaneously (2.5μg each) and FRGxCTLA-4 (5μg). After incubation for an additional 48 hours, cells were subjected to TUNEL evaluations and immunofluorescence evaluations of CD8, perforin, granzyme-B and PTEN by as described (Ma et al., 2021).

Quantification and Statistical analysis

Statistical evaluations were undertaken with GraphPad Prism software. As appropriate, groups were compared with 2-tailed Student's *t* test or with nonparametric Mann-Whitney *U* test. Values are expressed as mean ± SEM. One-way ANOVA with Turkey post hoc test was used for multiple group comparisons. Statistical significance was defined as a level of $P < 0.05$.

References

Attanasio, J., and E.J. Wherry. 2016. Costimulatory and Coinhibitory Receptor Pathways in Infectious Disease. *Immunity* 44:1052-1068.

Callahan, M.K., M.A. Postow, and J.D. Wolchok. 2016. Targeting T Cell Co-receptors for Cancer Therapy. *Immunity* 44:1069-1078.

Chen, C.C., J. Pekow, V. Llado, M. Kanneganti, C.W. Lau, A. Mizoguchi, M. Mino-Kenudson, M. Bissonnette, and E. Mizoguchi. 2011. Chitinase 3-like-1 expression in colonic epithelial cells as a potentially novel marker for colitis-associated neoplasia. *Am. J. Pathol.* 179:1494-1503.

Choi, I.K., Y.H. Kim, J.S. Kim, and J.H. Seo. 2010. High serum YKL-40 is a poor prognostic marker in patients with advanced non-small cell lung cancer. *Act Oncol* 49:861-864.

Cohen, J.V., and K.T. Flaherty. 2019. Response to Immune Checkpoint Antibodies: Not All Responses Are Created Equal. *Clin. Cancer Res.* 25:910.

Cohen, N., O. Shani, Y. Raz, Y. Sharon, D. Hoffman, L. Abramovitz, and N. Erez. 2017. Fibroblasts drive an immunosuppressive and growth-promoting microenvironment in breast cancer via secretion of Chitinase 3-like 1. *Oncogene* 36:4457-4468.

Dahlen, E., N. Veitonmaki, and P. Norlen. 2018. Bispecific antibodies in cancer immunotherapy. *Ther Adv Vaccines Immunother* 6:3-17.

Dela Cruz, C.S., W. Liu, C.H. He, A. Jacoby, A. Gornitsky, B. Ma, R.A. Flavell, C.G. Lee, and J.a. Elias. 2012. Chitinase 3-like-1 (Chi3l1) Regulation of Streptococcus pneumoniae Lung Infection. *Cell Host and Microbe* 12:34-46.

Dong, H., S.E. Strome, D.R. Salomao, H. Tamura, F. Hirano, D.B. Flies, P.C. Roche, J. Lu, G. Zhu, K. Tamada, V.A. Lennon, E. Celis, and L. Chen. 2002. Tumor-associated B7-H1 promotes T-cell apoptosis: a potential mechanism of immune evasion. *Nat. Med.* 8:793-800.

Duraiswamy, J., G.J. Freeman, and G. Coukos. 2014. Dual Blockade of PD-1 and CTLA-4 Combined with Tumor Vaccine Effectively Restores T-Cell Rejection Function in Tumors—Response. *Cancer Res.* 74:633.

Emerson, D.A., and W.L. Redmond. 2018. Overcoming Tumor-Induced Immune Suppression: From Relieving Inhibition to Providing Costimulation with T Cell Agonists. *Biodrugs* 32:221-231.

Esensten, J.H., Y.A. Helou, G. Chopra, A. Weiss, and J.A. Bluestone. 2016. CD28 Costimulation: From Mechanism to Therapy. *Immunity* 44:973-988.

He, C.H., C.G. Lee, C.S. Dela Cruz, C.M. Lee, Y. Zhou, F. Ahangari, B. Ma, E.L. Herzog, S.A. Rosenberg, Y. Li, A.M. Nour, C.R. Parikh, I. Schmidt, Y. Modis, L. Cantley, and J.A. Elias. 2013. Chitinase 3-like 1 regulates cellular and tissue responses via IL-13 receptor alpha2. *Cell Rep.* 4:830-841.

Heidegger, S., A. Wintges, F. Stritzke, S. Bek, K. Steiger, P.A. Koenig, S. Gottert, T. Engleitner, R. Ollinger, T. Nedelko, J.C. Fischer, V. Makarov, C. Winter, R. Rad, M.R.M. van den Brink, J. Ruland, F. Bassermann, T.A. Chan, T. Haas, and H. Poeck. 2019. RIG-I activation is critical for responsiveness to checkpoint blockade. *Sci Immunol* 4(39):eaau8943.

Hellmann, M.D., T.E. Ciuleanu, A. Pluzanski, J.S. Lee, G.A. Otterson, C. Audigier-Valette, E. Minenza, H. Linardou, S. Burgers, P. Salman, H. Borghaei, S.S. Ramalingam, J. Brahmer, M. Reck, K.J. O'Byrne, W.J. Geese, G. Green, H. Chang, J. Szustakowski, P. Bhagavatheeswaran, D. Healey, Y. Fu, F. Nathan, and L. Paz-Ares. 2018. Nivolumab plus Ipilimumab in Lung Cancer with a High Tumor Mutational Burden. *N. Engl. J. Med.* 378:2093-2104.

Herbst, R.S., J.C. Soria, M. Kowanetz, G.D. Fine, O. Hamid, M.S. Gordon, J.A. Sosman, D.F. McDermott, J.D. Powderly, S.N. Gettinger, H.E. Kohrt, L. Horn, D.P. Lawrence, S. Rost, M. Leabman, Y. Xiao, A. Mokatrin, H. Koeppen, P.S. Hegde, I. Mellman, D.S. Chen, and F.S. Hodi. 2014. Predictive correlates of response to the anti-PD-L1 antibody MPDL3280A in cancer patients. *Nature* 515:563-567.

Huff, W.X., J.H. Kwon, M. Henriquez, K. Fetcko, and M. Dey. 2019. The Evolving Role of CD8(+)CD28(-) Immunosenescent T Cells in Cancer Immunology. *Int. J. Mol. Sci.* 20:

Iwamoto, F.M., A.F. Hottinger, S. Karimi, E. Riedel, J. Dantis, M. Jahdi, K.S. Panageas, A.B. Lassman, L.E. Abrey, M. Fleisher, L.M. Deangelis, E.C. Holland, and A. Hormigo. 2011. Serum YKL-40 is a marker of prognosis and disease status in high-grade gliomas. *Neuro Oncol.* In Press:

Johansen, J.S., N.A. Schultz, and B.V. Jensen. 2009. Plasma YKL-40: A potential new cancer biomarker? *Future Oncol.* 5:1065-1082.

Junker, N., J.S. Johansen, C.B. Andersen, and P.E. Kristjansen. 2005. Expression of YKL-40 by peritumoral macrophages in human small cell lung cancer. *Lung Cancer* 48:223-231.

Kanneganti, M., M. Mino-Kenudson, and E. Mizoguchi. 2011. Animal models of colitis-associated carcinogenesis. *J. Biomed. Biotechnol.* 2011:342637.

Koyama, S., E.A. Akbay, Y.Y. Li, G.S. Herter-Sprie, K.A. Buczkowski, W.G. Richards, L. Gandhi, A.J. Redig, S.J. Rodig, H. Asahina, R.E. Jones, M.M. Kulkarni, M. Kuraguchi, S.

Palakurthi, P.E. Fecci, B.E. Johnson, P.A. Janne, J.A. Engelman, S.P. Gangadharan, D.B. Costa, G.J. Freeman, R. Bueno, F.S. Hodi, G. Dranoff, K.K. Wong, and P.S. Hammerman. 2016. Adaptive resistance to therapeutic PD-1 blockade is associated with upregulation of alternative immune checkpoints. *Nat Commun* 7:10501.

Larkin, J., V. Chiarion-Sileni, R. Gonzalez, J.J. Grob, C.L. Cowey, C.D. Lao, D. Schadendorf, R. Dummer, M. Smylie, P. Rutkowski, P.F. Ferrucci, A. Hill, J. Wagstaff, M.S. Carlino, J.B. Haanen, M. Maio, I. Marquez-Rodas, G.A. McArthur, P.A. Ascierto, G.V. Long, M.K. Callahan, M.A. Postow, K. Grossmann, M. Sznol, B. Dreno, L. Bastholt, A. Yang, L.M. Rollin, C. Horak, F.S. Hodi, and J.D. Wolchok. 2015. Combined Nivolumab and Ipilimumab or Monotherapy in Untreated Melanoma. *N. Engl. J. Med.* 373:23-34.

Lee, C.G., C.A. Da Silva, C.S. Dela Cruz, F. Ahangari, B. Ma, M.J. Kang, C.H. He, S. Takyar, and J.A. Elias. 2011. Role of chitin and chitinase/chitinase-like proteins in inflammation, tissue remodeling and injury. *Annu. Rev. Physiol.* 73:479-501.

Lee, C.G., D. Hartl, G.R. Lee, B. Koller, H. Matsuura, C.A. Da Silva, M.H. Sohn, L. Cohn, R.J. Homer, A.A. Kozhich, A. Humbles, J. Kearley, A. Coyle, G. Chupp, J. Reed, R.A. Flavell, and J.A. Elias. 2009. Role of breast regression protein 39 (BRP-39)/chitinase 3-like-1 in Th2 and IL-13-induced tissue responses and apoptosis. *J. Exp. Med.* 206:1149-1166.

Lee, C.M., C.H. He, A.M. Nour, Y. Zhou, B. Ma, J.W. Park, K.H. Kim, C. Dela Cruz, L. Sharma, M.L. Nasr, Y. Modis, C.G. Lee, and J.A. Elias. 2016. IL-13Ralpha2 uses TMEM219 in chitinase 3-like-1-induced signalling and effector responses. *Nat Commun* 7:12752.

Libreros, S., and V. Iragavarapu-Charyulu. 2015. YKL-40/CHI3L1 drives inflammation on the road of tumor progression. *J. Leukoc. Biol.* 98:931-936.

Ma, B., B. Akosman, S. Kamle, C.-M. Lee, C.H. He, J.S. Koo, C.G. Lee, and J.A. Elias. 2021. CHI3L1 regulates PD-L1 and anti–CHI3L1–PD-1 antibody elicits synergistic antitumor responses. *J. Clin. Invest.* 131:

Ma, B., E.L. Herzog, C.G. Lee, X. Peng, C.M. Lee, X. Chen, S. Rockwell, J.S. Koo, H. Kluger, R.S. Herbst, M. Sznol, and J.A. Elias. 2015. Role of chitinase 3-like-1 and semaphorin 7a in pulmonary melanoma metastasis. *Cancer Res.* 75:487-496.

Ma, B., E.L. Herzog, M. Moore, C.M. Lee, S.H. Na, C.G. Lee, and J.A. Elias. 2016. RIG-like Helicase Regulation of Chitinase 3-like 1 Axis and Pulmonary Metastasis. *Sci. Rep.* 6:26299.

Mahmoud, S.M., E.C. Paish, D.G. Powe, R.D. Macmillan, M.J. Grainge, A.H. Lee, I.O. Ellis, and A.R. Green. 2011. Tumor-infiltrating CD8+ lymphocytes predict clinical outcome in breast cancer. *J. Clin. Oncol.* 29:1949-1955.

Marcucci, F., C. Rumio, and A. Corti. 2017. Tumor cell-associated immune checkpoint molecules - Drivers of malignancy and stemness. *Biochim Biophys Acta Rev Cancer* 1868:571-583.

Matsuura, H., D. Hartl, M.J. Kang, C.S. Dela Cruz, B. Koller, G.L. Chupp, R.J. Homer, Y. Zhou, W.K. Cho, J.A. Elias, and C.G. Lee. 2011. Role of breast regression protein-39 in the pathogenesis of cigarette smoke-induced inflammation and emphysema. *Am. J. Respir. Cell Mol. Biol.* 44:777-786.

Motzer, R.J., N.M. Tannir, D.F. McDermott, O. Aren Frontera, B. Melichar, T.K. Choueiri, E.R. Plimack, P. Barthelemy, C. Porta, S. George, T. Powles, F. Donskov, V. Neiman, C.K. Kollmannsberger, P. Salman, H. Gurney, R. Hawkins, A. Ravaud, M.O. Grimm, S. Bracarda, C.H. Barrios, Y. Tomita, D. Castellano, B.I. Rini, A.C. Chen, S. Mekan, M.B. McHenry, M. Wind-Rotolo, J. Doan, P. Sharma, H.J. Hammers, B. Escudier, and I. CheckMate. 2018. Nivolumab plus Ipilimumab versus Sunitinib in Advanced Renal-Cell Carcinoma. *N. Engl. J. Med.* 378:1277-1290.

Nguyen, L.T., and P.S. Ohashi. 2015. Clinical blockade of PD1 and LAG3--potential mechanisms of action. *Nat. Rev. Immunol.* 15:45-56.

Ober, C., Z. Tan, Y. Sun, J.D. Possick, L. Pan, R. Nicolae, S. Radford, R.R. Parry, A. Heinzmann, K.A. Deichmann, L.A. Lester, J.E. Gern, R.F. Lemanske, Jr., D.L. Nicolae, J.A. Elias, and G.L. Chupp. 2008. Effect of variation in CHI3L1 on serum YKL-40 level, risk of asthma, and lung function. *N. Engl. J. Med.* 358:1682-1691.

Peng, C., J. Peng, L. Jiang, Q. You, J. Zheng, and X. Ning. 2010. YKL-40 protein levels and clinical outcome of human endometrial cancer. *J. Int. Med. Res.* 38:1448-1457.

Pfirschke, C., C. Engblom, S. Rickelt, V. Cortez-Retamozo, C. Garris, F. Pucci, T. Yamazaki, V. Poirier-Colame, A. Newton, Y. Redouane, Y.J. Lin, G. Wojtkiewicz, Y. Iwamoto, M. Mino-Kenudson, T.G. Huynh, R.O. Hynes, G.J. Freeman, G. Kroemer, L. Zitvogel, R. Weissleder, and M.J. Pittet. 2016. Immunogenic Chemotherapy Sensitizes Tumors to Checkpoint Blockade Therapy. *Immunity* 44:343-354.

Qin, S., L. Xu, M. Yi, S. Yu, K. Wu, and S. Luo. 2019. Novel immune checkpoint targets: moving beyond PD-1 and CTLA-4. *Mol. Cancer* 18:155.

Rotte, A. 2019. Combination of CTLA-4 and PD-1 blockers for treatment of cancer. *J. Exp. Clin. Cancer Res.* 38:255.

Rudd, C.E. 2009. CTLA-4 co-receptor impacts on the function of Treg and CD8+ T-cell subsets. *Eur. J. Immunol.* 39:687-690.

Santini, F.C., and M.D. Hellmann. 2018. PD-1/PD-L1 Axis in Lung Cancer. *Cancer J.* 24:15-19.

Schmidt, H., J.S. Johansen, J. Gehl, P.F. Geertsen, K. Fode, and H. von der Maase. 2006. Elevated serum level of YKL-40 is an independent prognostic factor for poor survival in patients with metastatic melanoma. *Cancer* 106:1130-1139.

Schumacher, T.N., and R.D. Schreiber. 2015. Neoantigens in cancer immunotherapy. *Science* 348:69.

Seidel, J.A., A. Otsuka, and K. Kabashima. 2018. Anti-PD-1 and Anti-CTLA-4 Therapies in Cancer: Mechanisms of Action, Efficacy, and Limitations. *Front. Oncol.* 8:86-86.

Shao, R., Q.J. Cao, R.B. Arenas, C. Bigelow, B. Bentley, and W. Yan. 2011. Breast cancer expression of YKL-40 correlates with tumour grade, poor differentiation, and other cancer markers. *Br. J. Cancer* 105:1203-1209.

Siegel, R.L., K.D. Miller, and A. Jemal. 2017. Cancer Statistics, 2017. *CA Cancer J. Clin.* 67:7-30.

Sohn, M.H., M.J. Kang, H. Matsuura, V. Bhandari, N.Y. Chen, C.G. Lee, and J.A. Elias. 2010. The chitinase-like proteins breast regression protein-39 and YKL-40 regulate hyperoxia-induced acute lung injury. *Am. J. Respir. Crit. Care Med.* 182:918-928.

Thom, I., B. Andritzky, G. Schuch, I. Burkholder, L. Edler, J.S. Johansen, C. Bokemeyer, U. Schumacher, and E. Laack. 2010. Elevated pretreatment serum concentration of YKL-40-An independent prognostic biomarker for poor survival in patients with metastatic nonsmall cell lung cancer. *Cancer* 116:4114-4121.

Topalian, S.L. 2017. Targeting Immune Checkpoints in Cancer Therapy. *JAMA* 318:1647-1648.

Topalian, S.L., C.G. Drake, and D.M. Pardoll. 2015. Immune checkpoint blockade: a common denominator approach to cancer therapy. *Cancer Cell* 27:450-461.

Wolchok, J.D., V. Chiarion-Sileni, R. Gonzalez, P. Rutkowski, J.J. Grob, C.L. Cowey, C.D. Lao, J. Wagstaff, D. Schadendorf, P.F. Ferrucci, M. Smylie, R. Dummer, A. Hill, D. Hogg, J. Haanen, M.S. Carlino, O. Bechter, M. Maio, I. Marquez-Rodas, M. Guidoboni, G. McArthur, C. Lebbe, P.A. Ascierto, G.V. Long, J. Cebon, J. Sosman, M.A. Postow, M.K. Callahan, D. Walker, L. Rollin, R. Bhore, F.S. Hodi, and J. Larkin. 2017. Overall Survival with Combined Nivolumab and Ipilimumab in Advanced Melanoma. *N. Engl. J. Med.* 377:1345-1356.

Xu, C., C.M. Fillmore, S. Koyama, H. Wu, Y. Zhao, Z. Chen, G.S. Herter-Sprie, E.A. Akbay, J.H. Tchaicha, A. Altabef, J.B. Reibel, Z. Walton, H. Ji, H. Watanabe, P.A. Jänne, D.H. Castrillon, A.K. Rustgi, A.J. Bass, G.J. Freeman, R.F. Padera, G. Dranoff, P.S. Hammerman, C.F. Kim, and K.K. Wong. 2014. Loss of Lkb1 and Pten leads to lung squamous cell carcinoma with elevated PD-L1 expression. *Cancer Cell* 25:590-604.

Yang, Y. 2015. Cancer immunotherapy: harnessing the immune system to battle cancer. *J. Clin. Invest.* 125:3335-3337.

Zhao, Y., C.K. Lee, C.-H. Lin, R.B. Gassen, X. Xu, Z. Huang, C. Xiao, C. Bonorino, L.-F. Lu, J.D. Bui, and E. Hui. 2019. PD-L1:CD80 Cis-Heterodimer Triggers the Co-stimulatory Receptor CD28 While Repressing the Inhibitory PD-1 and CTLA-4 Pathways. *Immunity* 51:1059-1073.e1059.

Zhao, Y., W. Yang, Y. Huang, R. Cui, X. Li, and B. Li. 2018. Evolving Roles for Targeting CTLA-4 in Cancer Immunotherapy. *Cell. Physiol. Biochem.* 47:721-734.

Zhou, Y., C.H. He, E.L. Herzog, X. Peng, C.M. Lee, T.H. Nguyen, M. Gulati, B.R. Gochuico, W.A. Gahl, M.L. Slade, C.G. Lee, and J.A. Elias. 2015. Chitinase 3-like-1 and its receptors in Hermansky-Pudlak syndrome-associated lung disease. *J. Clin. Invest.*

Figure Legends

Fig.1. Pulmonary melanoma metastasis inhibits T cell co-stimulation. WT mice were given B16-F10 (B16) melanoma cells or control vehicle (PBS) and evaluated 2 weeks later. (A-C) Real-time RT-PCR (RT-PCR) was used to quantitate the levels of mRNA encoding ICOS, ICOSL and CD28 in the lungs from mice treated intravenously with PBS (B16 -) or B16 cells (B16 +). Each dot represents an evaluation in an individual animal. (D) Western blot and densitometry evaluations of ICOS, ICOSL and CD28 accumulation in lungs from mice treated with PBS (B16-) or B16 cells (B16 +). (E and F) FACS evaluations quantitating the accumulation of ICOS and CD28 in cell populations from lungs of mice treated with B16 cells (B16+) or vehicle control (B16-). These evaluations used specific markers of airway myeloid cells. The values in panel A represent the mean±SEM of the noted evaluations. Panels D, E and F are representative of a minimum of 2 similar evaluations. *$P<0.05$, **$P<0.01$ (*t*-Test).

Fig.2. Chi3l1 plays a critical role in B16 melanoma stimulation of pulmonary CTLA-4 and its ligands. WT mice were given B16-F10 (B16) melanoma cells or control vehicle (PBS) and evaluated 2 weeks later. (A-C) RT-PCR was used to quantitate the levels of mRNA encoding CTLA-4, B7-1 and B72 in the lungs from mice treated intravenously with PBS vehicle (B16 -) or B16 cells (B16 +). Each dot represents an evaluation in an individual animal. (D) Western blot and densitometry evaluations of CTLA-4, B7-1 and B7-2 accumulation in lungs from WT mice treated with vehicle (B16-) or B16 cells (B16 +). (E and F) FACS analysis demonstrating the induction of CTLA-4 by CD11b+ and CD3+ cells. The plotted values in panels A-C represent the mean±SEM of the noted evaluations represented by the individual dots. Panels D and E are representative of a minimum of 2 similar evaluations. **$P<0.01$, ***$P<0.001$ (*t*-Test).

Fig.3. CHI3L1 plays a critical role in B16 cell regulation of T cell co-stimulators and the induction of CTLA-4 and its ligands. WT (*Chil1*$^{+/+}$) and Chi3l1 null (*Chil1*$^{-/-}$) mice were used to

evaluate the expression and accumulation of co-stimulators (ICOS, ICOS L CD28) and CTLA-4, B7-1 and B7-2 in the lung. (A) RT-PCR was used to quantitate the levels of mRNA encoding ICOS, ICOS L and CD28 in the lungs from WT mice and *Chil1*$^{-/-}$ mice randomized to receive B16 cells (B16+) or control vehicle (B16-). (B) RT-PCR was used to quantitate the levels of mRNA encoding CTLA-4, B7-1and B7-2 in the lungs from WT mice and *Chil1*$^{-/-}$ mice randomized to receive B16 cells (B16+) or control vehicle (B16-). (C and D) RT-PCR was used to quantitate the levels of mRNA encoding ICOS, ICOS L, CD28 CTLA-4, B7-1 and B7-2 in the lungs from WT mice randomized to receive B16 cells (B16+) or vehicle control (B16-) and randomized to receive the FRG antibody (FRG+) or an isotype antibody control (FRG-). (E) RT-PCR was used to quantitate the levels of mRNA encoding CTLA-4, B7-1 and B7-2 in the lungs from WT mice and Chi3l1 transgenic (*Chi3l1* Tg) mice randomized to receive B16 cells (B16+) or vehicle control (B16-). In all panels each dot represents the evaluation in an individual animal. The values in these panels represent the mean±SEM of the noted evaluations represented by the individual dots. **P*<0.05. ***P*<0,01, ****P*<0.005 (ANOVA with multiple comparisons).

Fig.4. Chi3l1 inhibits co-stimulation and stimulates pulmonary CTLA-4 in the normal lung. WT and Chi3l1 Tg (+) mice were used to evaluate the effects of transgenic Chi3l1 on co-stimulation and the CTLA-4 axis. (A) RT-PCR was used to quantitate the levels of mRNA encoding ICOS, ICOS L and CD28 in the lungs from WT mice and Chi3l1 Tg+ mice. (B) RT-PCR was used to quantitate the levels of mRNA encoding CTLA-4, B7-1and B7-2 in the lungs from WT mice and Chi3l1 Tg+ mice. (C) Western blot and densitometry evaluations of ICOS, ICOSL, CD28 B7-1 and B7-2 accumulation in lungs from WT and Chi3l1 Tg+ mice. (D) FACS evaluations quantitating the accumulation of CTLA-4 in CD3+ cells from WT mice and Chi3l1 Tg+ mice. (E) Cumulative FACS evaluations quantitating the accumulation of CTLA-4 in CD3+ cells from WT and Chi3l1 Tg+ mice. The plotted values in panels A, B and E represent the mean ± SEM of the noted evaluations represented by the individual dots. Panel C is representative of a minimum of

2 similar evaluations. *P<0.05, **P<0.01 (t-Test for panels A and B, ANOVA with multiple comparisons for panels E).

Fig.5. Rig-like helicase (RLH) activation augments co-stimulation and inhibits CTLA-4, B7-1 and B7-2. WT mice were used to evaluate the effects of Rig-like helicase activation with Poly (I:C) on co-stimulation and the CTLA-4 axis. (A) RT-PCR was used to quantitate the levels of mRNA encoding ICOS, ICOS L and CD28 in the lungs from WT mice that received B16 cells (B16+) or vehicle control (B16-) and were treated with Poly (I:C) (+) or its vehicle control (Poly(I:C)-). (B) RT-PCR was used to quantitate the levels of mRNA encoding CTLA-4, B7-1 and B7-2 in the lungs from WT mice that received B16 cells (B16+) or vehicle control (B16-) and were treated with Poly (I:C) (+) or its vehicle control (Poly(I:C)-). (C) FACS evaluations comparing the expression of CTLA-4 on CD3+ cells from WT mice that received B16 cells (B16+) or vehicle control (B16-) and were treated with Poly (I:C) or its vehicle control. (D) FACS evaluations comparing the expression of CD28 on CD11b+ cells from WT mice that received B16 cells (B16+) or vehicle control (B16-) and were treated with Poly (I:C) or its vehicle control. The plotted values in panels A and B represent the mean ± SEM of the noted evaluations represented by the individual dots. Panels C and D are representative of a minimum of 2 similar evaluations. *P<0.05, **P<0.01, ***P<0.001 (ANOVA with multiple comparisons).

Fig. 6. Effects of transgenic Chi3l1 on Rig-like helicase (RLH) inhibition of co-stimulation and induction of CTLA-4, B7-1 and B7-2. WT mice and Chi3l1 Tg+ mice were given B16-F10 (B16+) melanoma cells or PBS control (B16-) and treated with Poly(I:C) (Poly (I:C+) or its vehicle control (Poly(I:C-) and evaluated 2 weeks later. (A-F) RT-PCR was used to quantitate the levels of mRNA encoding ICOS, ICOSL, CD28, CTLA-4, B7-1 and B7-2 in lungs from WT mice and Chi3l1 Tg+ mice treated with Poly(I:C) (Poly (I:C+) or its vehicle control (Poly (I:C-) as noted. The plotted values in panels A-F represent the mean±SEM of the evaluations represented by the

individual dots. *P<0.05, **P<0.01, ***P<0.001. (ANOVA with multiple comparisons). ns, not significant.

Fig. 7. Anti-Chi3l1 and anti-CTLA-4 interact to augment antitumor responses in melanoma lung metastasis. WT mice were given B16-F10 (B16) melanoma cells or control vehicle and treated with control IgG, FRG and or anti-CTLA-4 antibodies, alone or in combination, and melanoma lung metastasis was evaluated 2 weeks later. (A) Representative lungs from mice treated with control IgG, FRG and or anti-CTLA-4 antibodies, alone or in combination. They were compared to the mice treated with indicated doses of the bispecific antibody FRG-CTLA-4. As noted, the antibodies were given at doses of 100μg or 50 μg every other day by intra-peritoneal injection. (B) The number of pleural melanoma colonies was quantitated in the lungs from the mice in panel A. Each dot is representative of an individual animal. Panel A is a representative of at least 3 evaluations. The values in panel B represent the mean±SEM of the evaluations represented by the individual dots in the lungs from the experiment representatively illustrated in panel A. *P<0.05. ***P<0.001; ****P<0.0001. (ANOVA with multiple comparisons).

Fig.8. Bispecific antibodies that simultaneously target Chi3l1 and CTLA-4 induce synergistic CTL- mediated tumor cell death responses and tumor cell PTEN expression. The antitumor effects of the FRGxCTLA-4 bispecific antibody were evaluated in a co-culture system containing TALL-104 cells and A375 human melanoma cells. TALL-104 cells were activated by pretreatment with anti-CD3 and anti-CD28 (1 μg/ml each and incubated for 2 hrs in 5% CO2 and air at 37°C). The TALL-104 cells were then co-cultured with A357 human melanoma cells for 24 hours. These co-cultures were undertaken in the presence of the following antibodies; isotype control antibody (5μg/ml), anti-CTLA-4 or anti-Chi3l1 (FRG) alone (5μg/ml), or in combination (2.5 μg/ml each), and the bispecific FRGxCTLA-4 antibody (5μg/ml). (Column A) Representative demonstration and quantitation of apoptotic tumor cell death using in situ cell

detection kit -fluorescein dUTP. TUNEL (+) cells stain green. (Columns B-D) Representative demonstration and quantification of TALL-104 cell expression of CD8 (B), perforin (C) and granzyme (D). Tumor cells are green and positive staining TALL-104 cells are yellow-orange. (E) Representative demonstration and quantification of tumor cell PTEN. Tumor cells are green and PTEN is yellow-orange. (Row F) Quantification of the evaluations in A-E. The % of TUNEL + tumor cells (Column A), % of TALL-104 cells expressing CD8 (column B), perforin (column C) and granzyme (column D) and % of tumor cells expressing PTEN (column E) are illustrated. These evaluations were done using fluorescent microscopy (x20 of original magnification). In these quantifications, 5 randomly selected fields were evaluated. The values in panel F are the mean$\pm$SEM. ***$P<0.001$, ****$P<0.0001$. Scale bar =10μm, applies to all subpanels of A-E.

Fig. 1

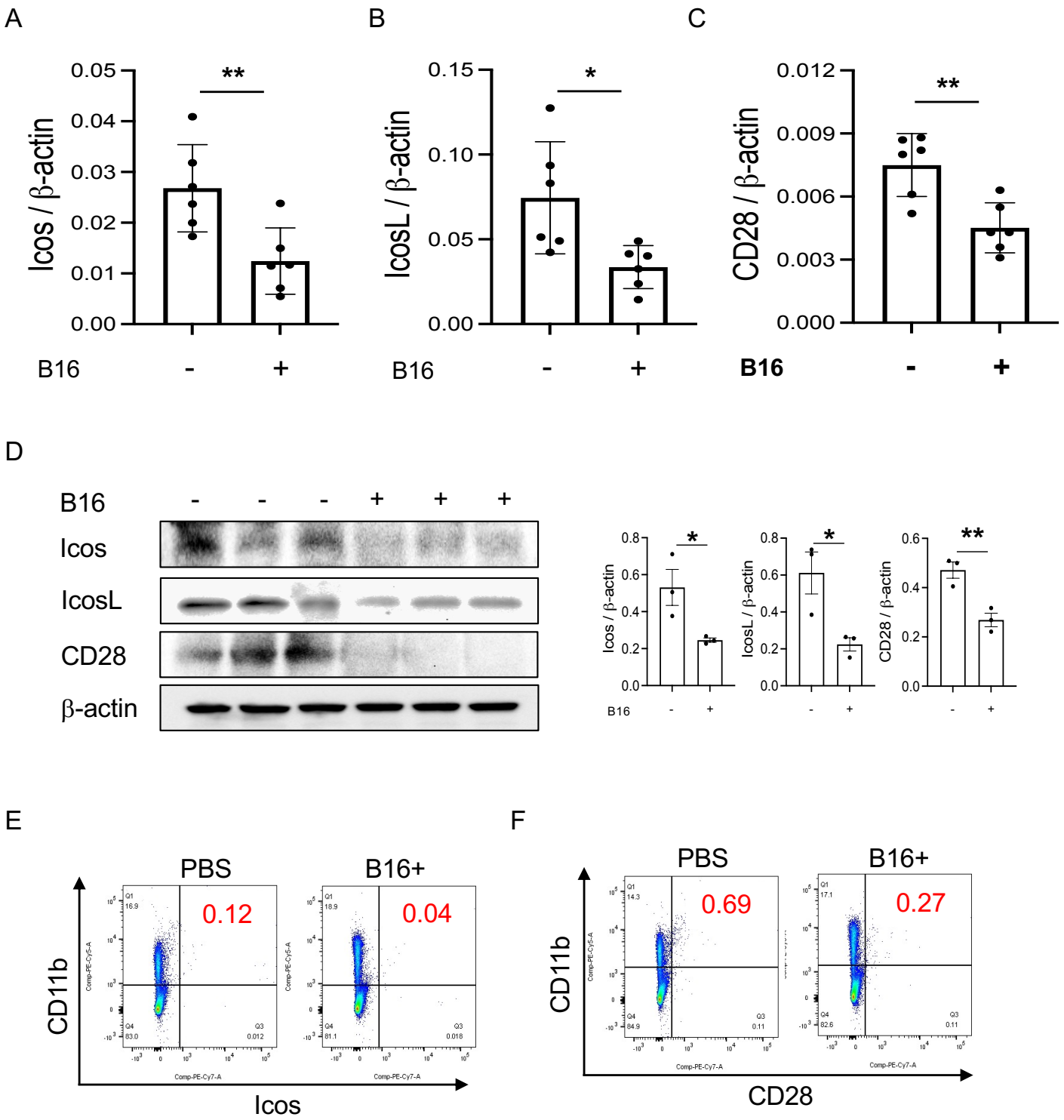
A
B
C
Icos / β-actin
IcosL / β-actin
CD28 / β-actin
B16
-
+
D
Icos
IcosL
CD28
β-actin
E
F
PBS
B16+
0.12
0.04
0.69
0.27
CD11b
Icos
CD28

Fig. 2

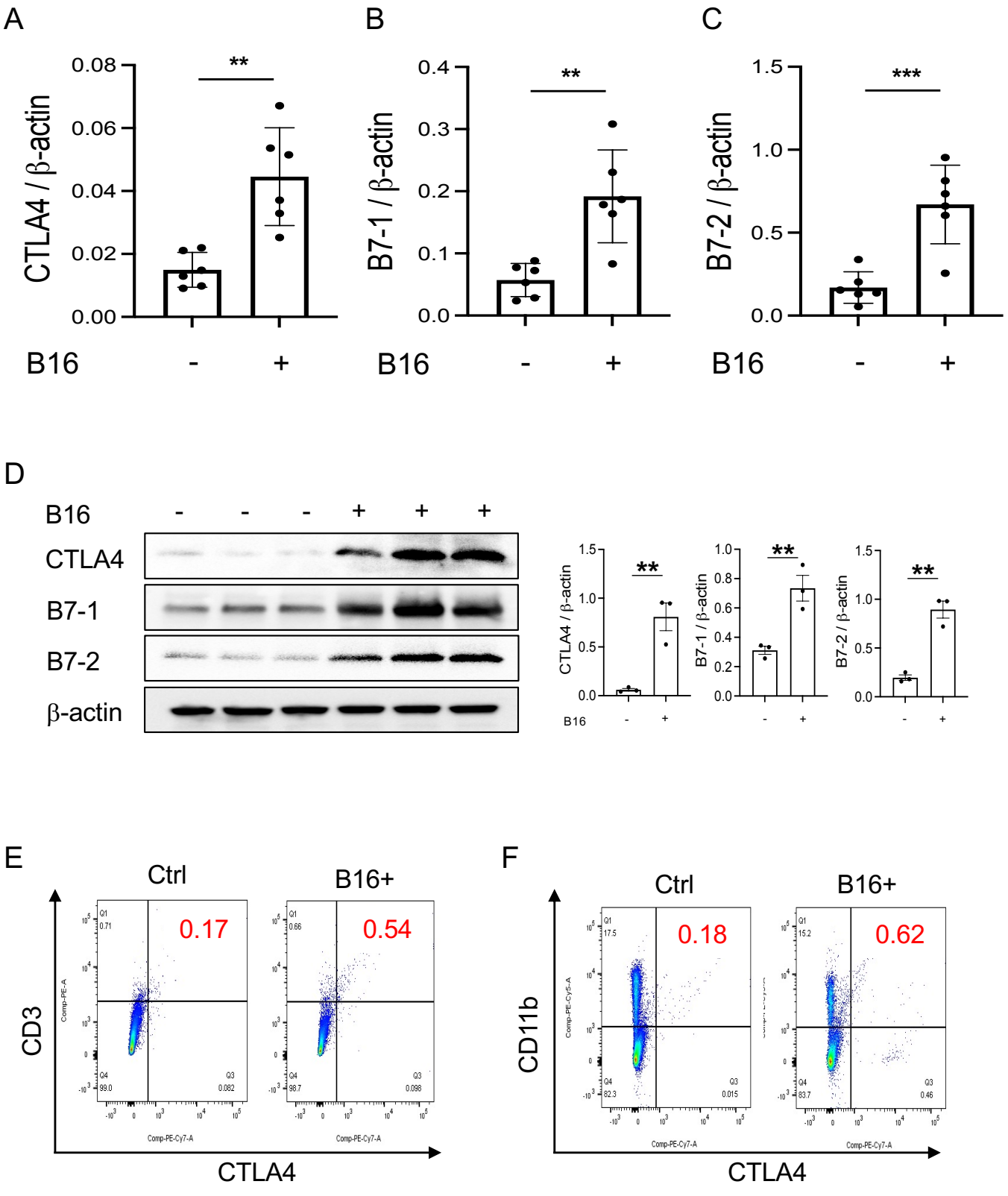
A
CTLA4 / β-actin
0.08
0.06
0.04
0.02
0.00
**
B16
-
+
B
B7-1 / β-actin
0.4
0.3
0.2
0.1
0.0
**
B16
-
+
C
B7-2 / β-actin
1.5
1.0
0.5
0.0
***
B16
-
+
D
B16
- - - + + +
CTLA4
B7-1
B7-2
β-actin
CTLA4 / β-actin
B7-1 / β-actin
B7-2 / β-actin
**
B16
E
Ctrl
B16+
0.17
0.54
CD3
CTLA4
F
Ctrl
B16+
0.18
0.62
CD11b
CTLA4

Fig. 3

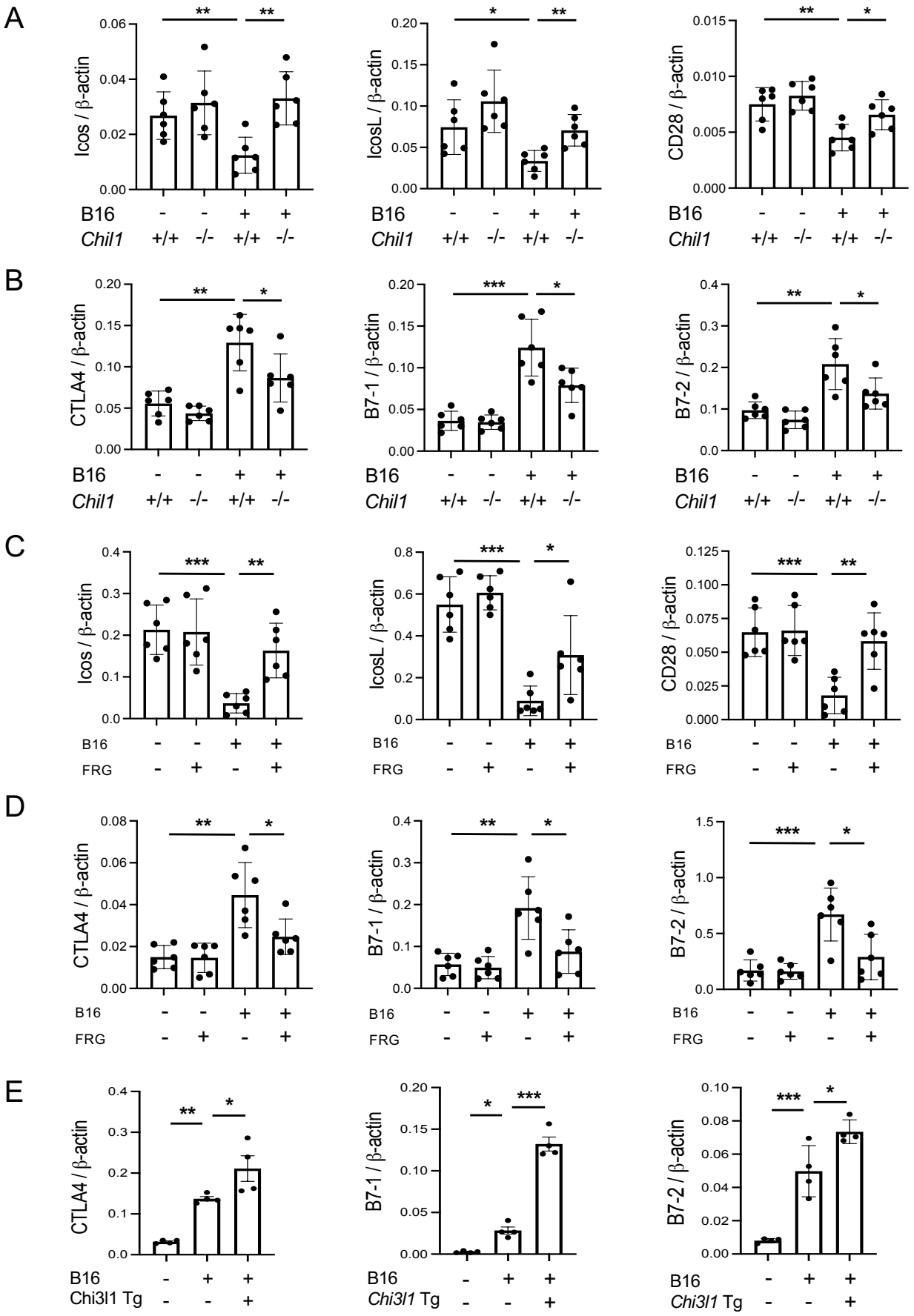
A
Icos / β-actin
IcosL / β-actin
CD28 / β-actin
B16 - - + +
Chil1 +/+ -/- +/+ -/-
B
CTLA4 / β-actin
B7-1 / β-actin
B7-2 / β-actin
B16 - - + +
Chil1 +/+ -/- +/+ -/-
C
Icos / β-actin
IcosL / β-actin
CD28 / β-actin
B16 - - + +
FRG - + - +
D
CTLA4 / β-actin
B7-1 / β-actin
B7-2 / β-actin
B16 - - + +
FRG - + - +
E
CTLA4 / β-actin
B7-1 / β-actin
B7-2 / β-actin
B16 - + +
Chi3l1 Tg - - +
B16 - + +
Chi3l1 Tg - - +

Fig. 4

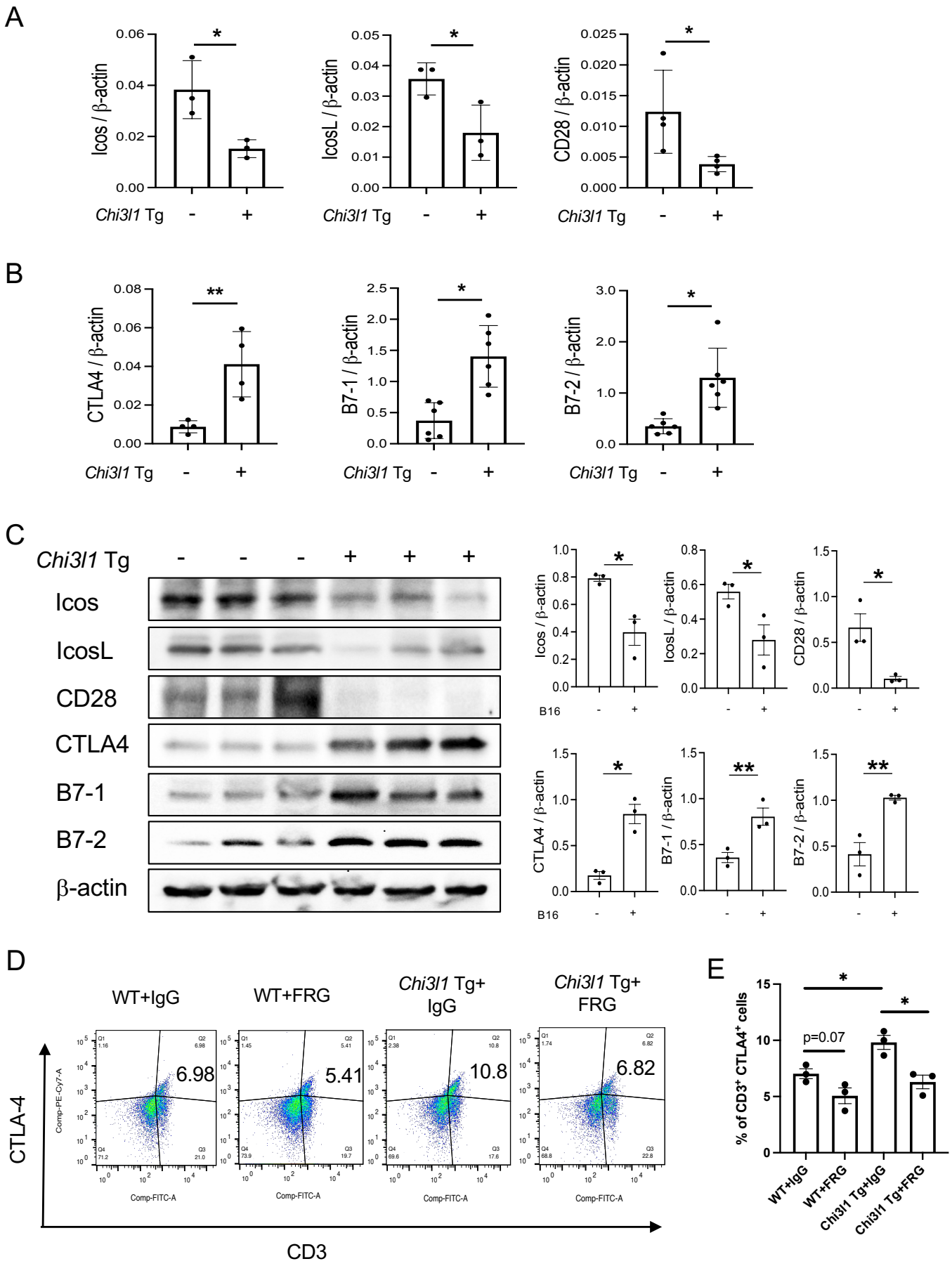
A
Icos / β-actin
IcosL / β-actin
CD28 / β-actin
Chi3l1 Tg - +
B
CTLA4 / β-actin
B7-1 / β-actin
B7-2 / β-actin
C
Chi3l1 Tg - - - + + +
Icos
IcosL
CD28
CTLA4
B7-1
B7-2
β-actin
B16 - +
D
WT+IgG
WT+FRG
Chi3l1 Tg+ IgG
Chi3l1 Tg+ FRG
6.98
5.41
10.8
6.82
CTLA-4
CD3
Comp-PE-Cy7-A
Comp-FITC-A
E
% of CD3+ CTLA4+ cells
p=0.07
WT+IgG
WT+FRG
Chi3l1 Tg+IgG
Chi3l1 Tg+FRG

Fig. 5

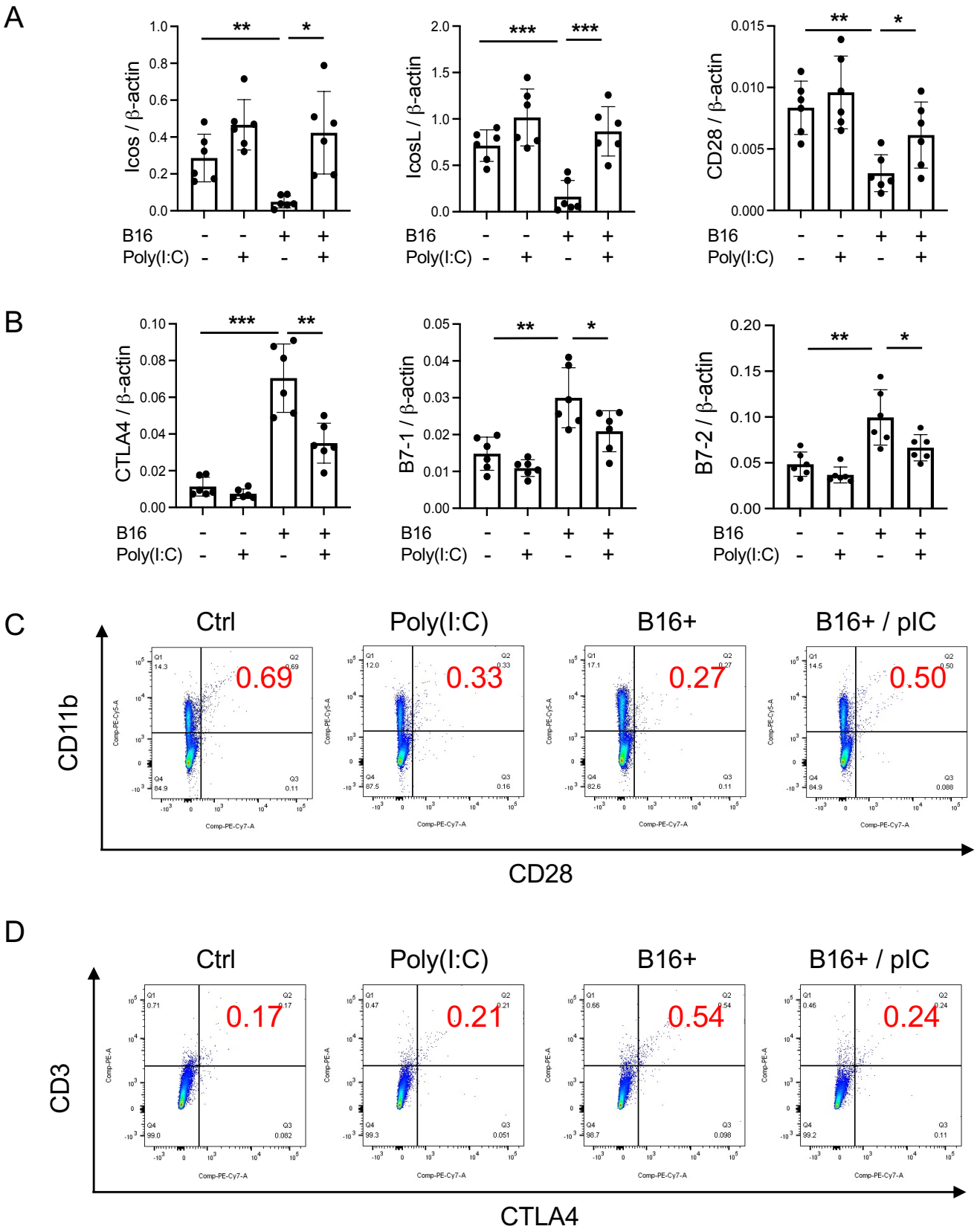
A
Icos / β-actin
IcosL / β-actin
CD28 / β-actin
B16
Poly(I:C)
B
CTLA4 / β-actin
B7-1 / β-actin
B7-2 / β-actin
C
Ctrl
Poly(I:C)
B16+
B16+ / pIC
0.69
0.33
0.27
0.50
CD11b
CD28
D
0.17
0.21
0.54
0.24
CD3
CTLA4

Fig. 6

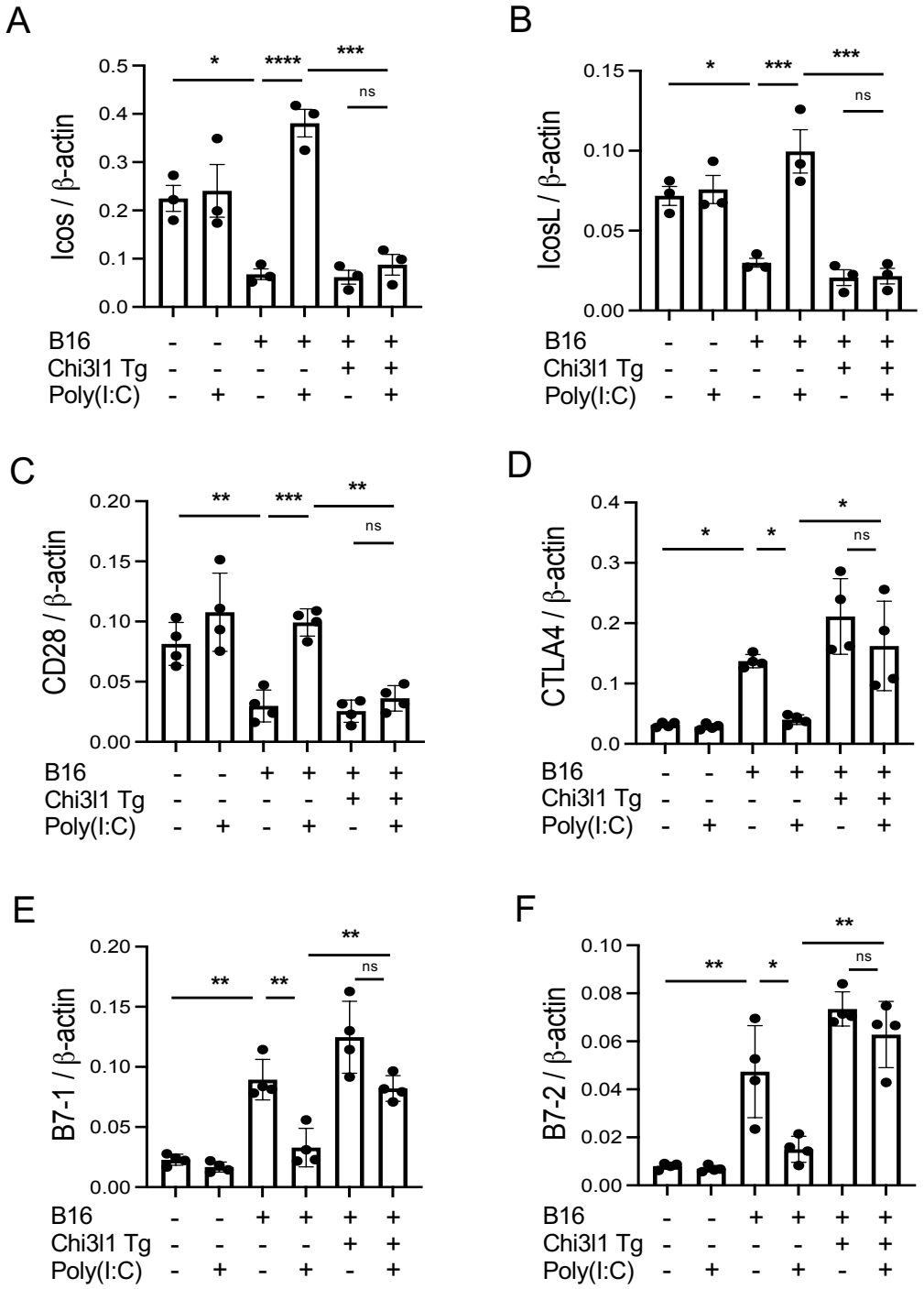
A
Icos / β-actin
0.5
0.4
0.3
0.2
0.1
0.0
*
****
***
ns
B16 - - + + + +
Chi3l1 Tg - - - - + +
Poly(I:C) - + - + - +
B
IcosL / β-actin
0.15
0.10
0.05
0.00
*
***
***
ns
B16 - - + + + +
Chi3l1 Tg - - - - + +
Poly(I:C) - + - + - +
C
CD28 / β-actin
0.20
0.15
0.10
0.05
0.00
**
***
**
ns
B16 - - + + + +
Chi3l1 Tg - - - - + +
Poly(I:C) - + - + - +
D
CTLA4 / β-actin
0.4
0.3
0.2
0.1
0.0
*
*
*
ns
B16 - - + + + +
Chi3l1 Tg - - - - + +
Poly(I:C) - + - + - +
E
B7-1 / β-actin
0.20
0.15
0.10
0.05
0.00
**
**
**
ns
B16 - - + + + +
Chi3l1 Tg - - - - + +
Poly(I:C) - + - + - +
F
B7-2 / β-actin
0.10
0.08
0.06
0.04
0.02
0.00
**
*
**
ns
B16 - - + + + +
Chi3l1 Tg - - - - + +
Poly(I:C) - + - + - +

Fig. 7

A

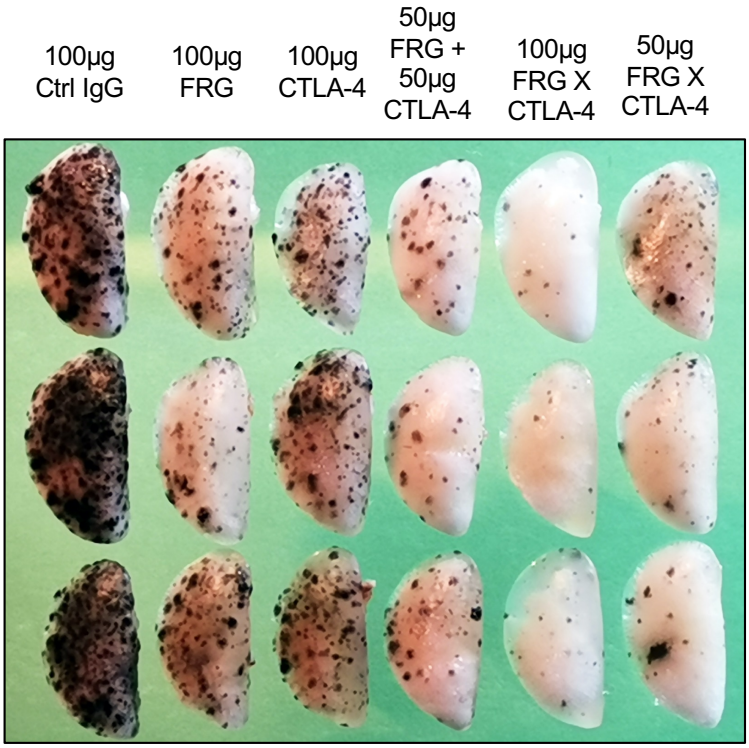
100µg Ctrl IgG
100µg FRG
100µg CTLA-4
50µg FRG + 50µg CTLA-4
100µg FRG X CTLA-4
50µg FRG X CTLA-4

B

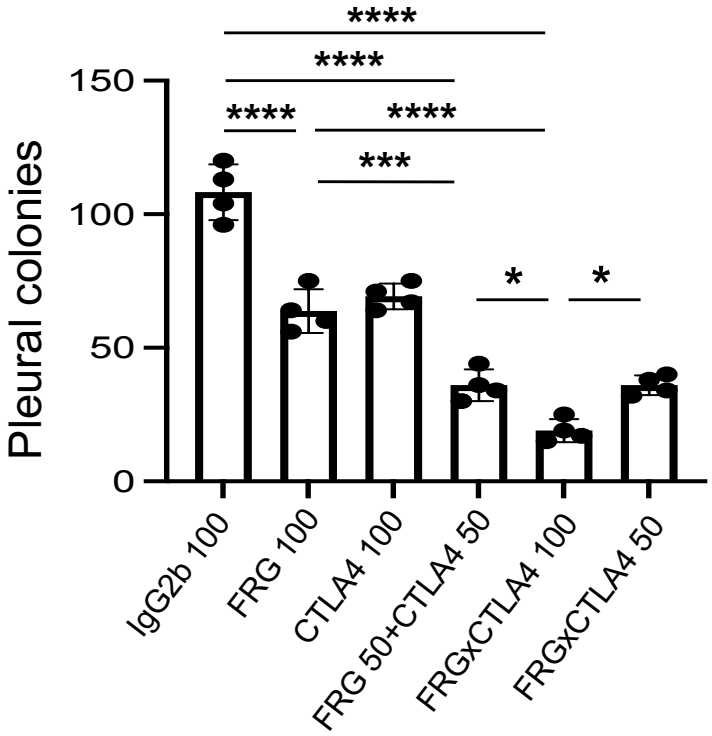
Pleural colonies
150
100
50
0
****
****
****
****
***
*
*
IgG2b 100
FRG 100
CTLA4 100
FRG 50+CTLA4 50
FRGxCTLA4 100
FRGxCTLA4 50

Fig. 8

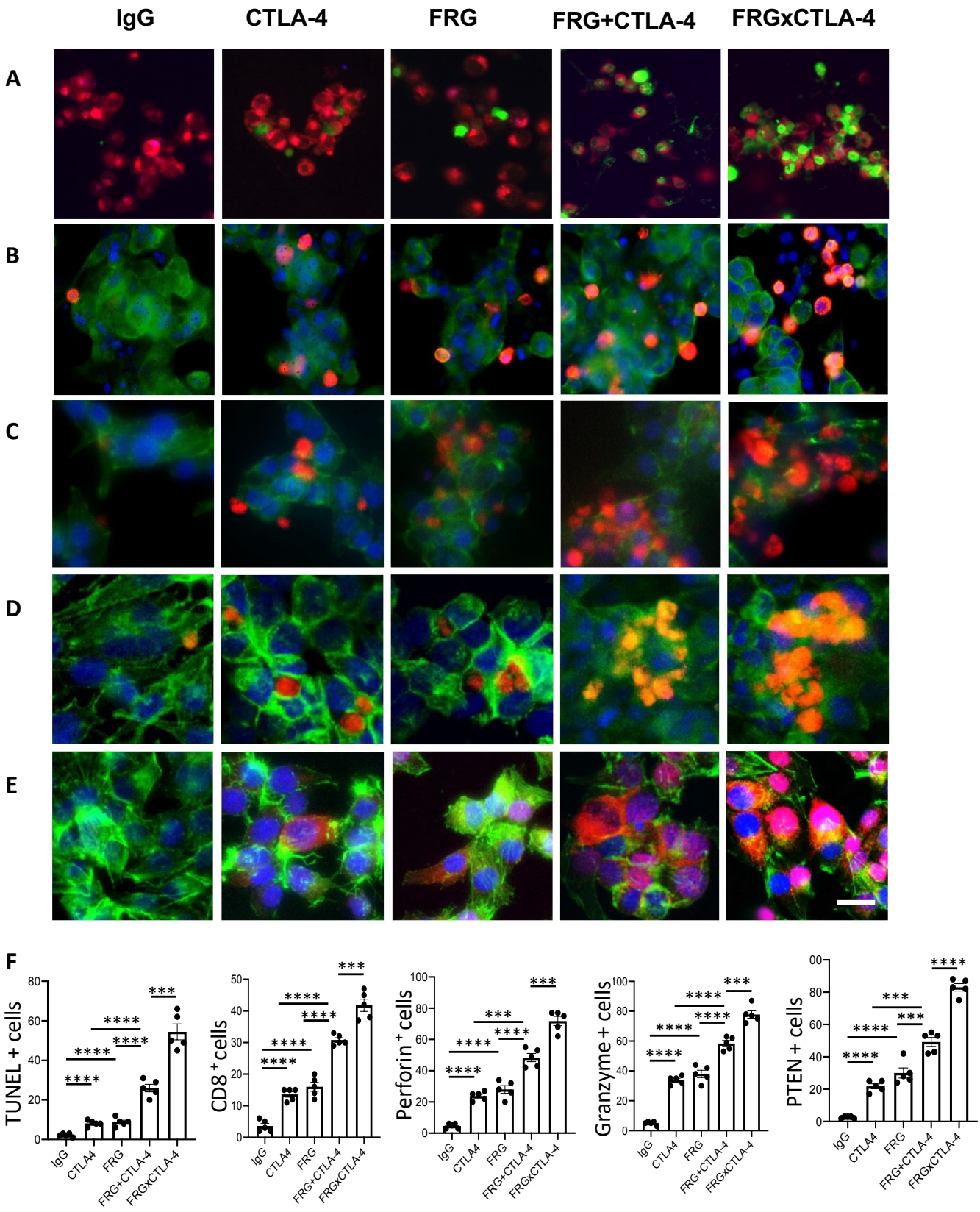
IgG
CTLA-4
FRG
FRG+CTLA-4
FRGxCTLA-4
A
B
C
D
E
F
TUNEL + cells
CD8+ cells
Perforin+ cells
Granzyme + cells
PTEN + cells
IgG
CTLA4
FRG
FRG+CTLA-4
FRGxCTLA-4
****
***